H/Br Exchange in BBr_3 by $HSiR_3$ (R = H, CH_3, C_2H_5): Origin of DFT Failures to Describe a Seemingly Innocuous Reaction Barrier†

Julia R. Rakow, Sandor Tüllmann, and Max C. Holthausen*

Institut für Anorganische Chemie, Johann Wolfgang Goethe-Universität Frankfurt am Main, Max-von-Laue-Str. 7, D-60438 Frankfurt am Main, Germany

Received: July 10, 2009; Revised Manuscript Received: September 16, 2009

We investigate the suitability of density functional theory (DFT) and second order Møller−Plesset perturbation theory (MP2) for the title reaction, which serves as a model to represent the key step in a recently developed B−C bond formation reaction. CBS-QB3 is employed as a reference throughout this study. The classical barrier height associated with the concerted transition state for the H/Br exchange reaction poses a serious challenge to most standard GGAs or hybrid functionals. In particular the popular B3LYP hybrid functional shows dramatically overestimated reaction barriers (by 12 kcal mol^{-1}) for the largest system with R = C_2H_5. We find that a proper description of intramolecular dispersion interactions arising in the transition state is crucial for a correct assessment of this reaction and that the inclusion of Grimme's empirical dispersion correction effectively compensates for most of the errors to a large extent. In conclusion we find a pleasing performance of the dispersion corrected functionals B2PLYP-D or B3LYP-D for the present set of systems if used in combination with basis sets of triple-ζ quality, which we recommend for future quantum chemical studies on related systems. Also the recently devised M05−2X hybrid meta-GGA shows an excellent performance, in particular if used in combination with the small SVP basis.

1. Introduction

The chemistry of organoboron polymers is a field of growing interest due to the unusual electronic properties of materials containing π-conjugated spacer moieties that enable electronic communication across three-coordinate boron centers providing vacant p orbitals for conjugative interactions. Such materials have potential applications, e.g., in optoelectronic devices or sensor materials research.[1,2] Further immediate interest in organoborane chemistry is spurred by the recent observation of Stephan and co-workers that BR_3/PR_3 Lewis acid/base pairs are able to reversibly activate H_2 under mild conditions.[3] Accordingly, the synthesis of related organoboron building blocks has moved into the focus of synthetic chemists. The most challenging step in the preparation of such compounds is the formation of the B−C bond(s). Nucleophilic substitution reactions involving organolithium or Grignard reagents are generally difficult to stop at the desired borane stage and tend to proceed instead to the tetracoordinate borate anion. To date, only a few synthetic pathways to such compounds have been developed.[4−7] Recently, Wagner and co-workers developed a novel condensation reaction based on the initial observation that borylated ferrocene[8] $FcBBr_2$ undergoes a coupling reaction upon treatment with $HSiEt_3$ to form quantitatively and selectively the diferrocenylborane Fc_2BBr (Fc = $(C_5H_5)Fe(C_5H_4)$) (Figure 1a).[9] This reaction has recently been extended to the preparation of high-molecular-weight boranediyl bridged polyferrocenylenes $[-fcB(Br)-]_n$ (Figure 1b) and to the preparation of polymeric 9,10-dihydro-9,10-diboraantracene (Figure 1c), which serves as an efficient precursor for boron-doped π-conjugated polymers.[10−12]

For a detailed understanding of these reactions, we have investigated the underlying elementary steps and electronic properties of this class of compounds previously by quantum chemical means.[13,14] In particular, we identified a concerted transition state for the initial H/Br exchange at the boron center by triethylsilane as a rate limiting step in the overall mechanism of the coupling reaction according to eq 1.

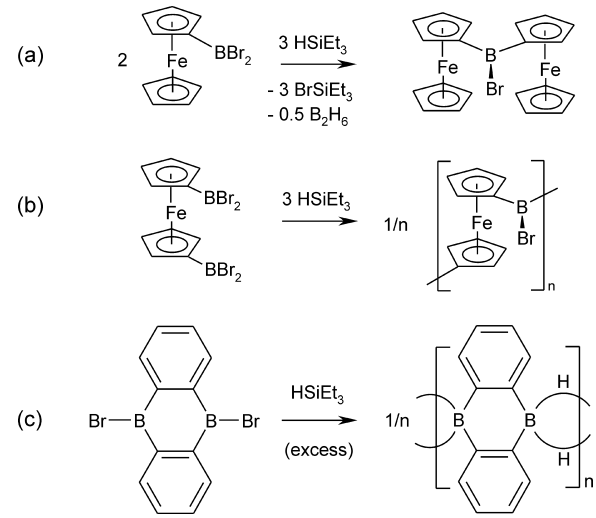

Figure 1. Reactions investigated earlier that involve H/Br exchange after treatment of reactants with $HSiEt_3$.

$$FcBBr_2 + HSiEt_3 \rightarrow FcBBrH + BrSiEt_3 \qquad (1)$$

The present study is motivated by our observation that all flavors of density functional theory (DFT) applied to this system resulted in dramatically overestimated barriers for the initial steps of the polymerization reaction, irrespective of the type of functional (GGA or hybrid) or the quality of basis set used.

† Part of the "Walter Thiel Festschrift".

* To whom correspondence should be addressed. E-mail: Max.Holthausen@chemie.uni-frankfurt.de. Phone: +49 69 798 29412. Fax: +49 69 798 29417.

10.1021/jp906502y CCC: $40.75
Published on Web 09/25/2009

Although we were able to perform quantum chemical calculations that provide sufficient accuracy in our former works, the methods applied were computationally rather demanding. As we plan to extend our cooperative studies on related systems in the future, we decided to systematically investigate the performance of available quantum chemical methods that are accurate but at the same time efficient enough to address also larger molecular sizes.

For any researcher experienced in theoretical studies on chemical reactivity, it comes as no surprise that DFT can fail to describe both relative stabilities and barrier heights in a balanced way. It is actually well-known that the performance of DFT strongly depends on the nature of systems being studied and usually shows large variations with the exchange-correlation functional chosen.[15] In particular the reliable description of classical barrier heights can pose severe challenges for otherwise well-performing functionals.[16−19] As such failures are often hard to predict, adequate use of DFT usually requires some pragmatic efforts to identify the optimum functional/basis set combination for each new class of chemical system studied.

One well-known deficiency of DFT is the complete neglect of long-range correlation effects underlying dispersive interactions in current local or semilocal density functionals. Since we found a strong dependence of the DFT performance on the system size (see below) we suspected that this issue might be a major source of the errors observed in our previous study. Yet, additional fundamental problems of DFT have been identified recently that cast even further doubts on the suitability of popular density functionals in particular for the class of systems under study: several groups have shown that B3LYP and other popular functionals seriously fall short to describe dative bonding in amine-borane Lewis acid/base complexes $R_3B \leftarrow NR'_3$,[20−22] depending on the degree of alkylation at B or N. Others were tossed at the same time with notorious shortcomings of DFT in the description of stereoelectronic effects that have come to light.[23−27] Grimme has argued convincingly that both, not obviously related, problems can be traced back to a general failure of standard functionals to properly account for medium-range pair correlation effects.[24,28] Within the context of DFT, three promising lines of recent developments can be pursued to overcome these problems: empirical dispersion corrections,[29−33] adequately parametrized hybrid (meta-) GGAs,[19,23,34,35] or double hybrid functionals[24,36,37] that account well for medium range nonbonding interactions.

Herein we provide a systematic assessment of the quality of various quantum chemical methods for the description of the key reaction step of the formation of functionalized organoboron species, i.e., the hydride transfer step from the silane to the borane. The aim of this study is to document dramatic problems of widely used exchange-correlation functionals with a seemingly innocuous reaction and to identify alternative theoretical procedures with acceptable cost/accuracy ratio that are applicable for related reactivity studies also on larger molecular systems. To this end we investigate the H/Br exchange reaction in BBr_3 by $HSiR_3$ (R = H, CH_3, C_2H_5) according to eq 2 as the parent molecular model system that contains many relevant structural and electronic features to represent a whole class of molecular building blocks employed in contemporary research in the field. At the same time, it is sufficiently small to assess the quality of quantum chemical methods by comparison to high-level post-HF data. We considered classical barrier heights only; that is, we did not take tunnel effects into account, which would reduce the activation barriers connected with this H-transfer step to some extent.

Three different silanes were chosen to scrutinize the influence of the system size on the computed reaction barriers.

$$HSiR_3 + BBr_3 \rightarrow BrSiR_3 + BHBr_2 \qquad (R = H, CH_3, C_2H_5) \tag{2}$$

We note in passing that in the experiments addition of further silane equivalents leads to complete H/Br exchange and subsequent dimerization of the resulting borane does provide an additional thermodynamic driving force for the overall reaction (B_2H_6 has been observed as side product for the overall reaction according to eq 1).[13] Here we concentrate, however, on the initial reaction sequence with one H/Br exchange step only and we do not consider any subsequent reaction steps.

2. Computational Details

Ab initio molecular orbital theory and DFT calculations were carried out with the Gaussian 03,[38] Molpro,[39] Turbomole,[40] and Orca[41] computer programs. The CBS-QB3 extrapolation scheme of Petersson and co-workers[42,43] was chosen as the benchmark method for all systems studied here. At the DFT level, we employed the functionals BP86,[44,45] BLYP,[46,47] PW91,[48,49] mPW91PW91,[50] B3LYP,[45,46,51,52] PBE,[53] PBE0 (dubbed PBE1PBE in Gaussian 03),[54,55] B98,[56] BMK,[19] M05,[57] and M05−2X[34] as implemented in the Gaussian 03 program. Additional calculations were performed with the mPWB1K[58] and X3LYP[35] functionals and with the recently devised double hybrid functional B2PLYP.[59] Grimme's empirical dispersion correction (DFT-D)[60] was used in combination with the B3LYP, PBE, and B2PLYP functionals (referred to as B3LYP-D, PBE-D, and B2PLYP-D); all three functionals and dispersion correction parameters were used as implemented in the Turbomole and Orca programs.[61] MP2, spin-component scaled MP2 (SCS-MP2),[62] and DFT single-point calculations have been performed using the Turbomole and Molpro programs. Unless noted otherwise, all DFT results refer to geometries fully optimized at the respective levels of theory. We used the Gaussian03 'external' facility in combination with a *Gau_External* module that we developed to drive geometry optimizations with Turbomole or Orca employed as quantum chemical engines providing energies and gradients. Unless noted otherwise, all stationary points were characterized correctly as minima or transition states by analysis of Hessian matrices obtained analytically or from numerical differentiation of gradients. In all calculations with the Orca program we used the *TightSCF*, *NoFinalGrid*, and *Grid4* options/cutoffs; the RIJONX approach[63,64] was used together with the SV/J and TZV/J auxiliary basis sets[65,66] for B3LYP calculations (SV/C and TZV/C auxiliary basis sets[67] for RI-B2PLYP calculations). Geometry optimizations and frequency calculations have been performed with the 6-31G(d) split-valence basis set,[68] the SVP,[62] and TZVP[69,70] basis sets.[71] The correlation consistent basis sets of Dunning and co-workers, (aug-)cc-pVXZ (X = D, T, Q, 5),[72,73] have been employed for CCSD(T), MP2, and some DFT calculations. CCSD(T), MP2, and B2PLYP single-point energies obtained with the aug-cc-pVXZ (X = D, T, Q, 5) basis sets have been extrapolated to the basis set limit (denoted xtra) using the Ansatz of Halkier et al.[74,75] for the correlation energy

$$E_{xtra(XY)} = E_Y^{HF} + (X^3 \cdot E_X^{corr} - Y^3 \cdot E_Y^{corr})/(X^3 - Y^3) \tag{3}$$

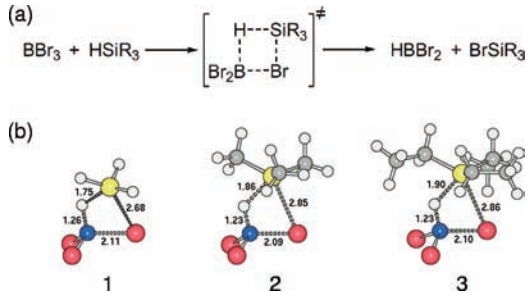

Figure 2. (a) Schematic representation of the reaction step (cf. eq 2) and (b) optimized transition state structures (**1**: R = H; **2**: R = CH_3; **3**: R = C_2H_5; B3LYP/TZVP optimized structures, bond lengths in Å; H: light gray; B: blue; C: gray; Si: yellow; Br: red).

where X and Y are the cardinal numbers of the correlation consistent basis sets ($D = 2$; $T = 3$; $Q = 4$; Y > X). B2PLYP and M05−2X results have alternatively been extrapolated to the basis set limit according to a mixed Gaussian/exponential Ansatz of Peterson et al.[76]

$$E_X = E_{xtra} + Ae^{-(X-1)} + Be^{-(X-1)^2}$$

Solving for E_{xtra} we obtained the following explicit expression to extrapolate total electronic energies to the basis set limit for cardinal numbers $X = \{2, 3, 4\}$

$$E_{xtra(DTQ)} = \frac{(e^4 - 1)E_D + (e - e^7)E_T + (e^8 - e^6)E_Q}{e^8 - e^7 - e^6 + e^4 + e - 1}$$

To assess the potential influence of relativistic effects due to the presence of Br, second-order scalar relativistic corrections have been evaluated in exemplary B2PLYP calculations employing the spin-free Douglas−Kroll−Hess Hamiltonian.[77−80] The DKH keyword in Orca was used, which automatically invokes partly decontracted SVP and TZVP basis sets designed for all-electron relativistic calculations. The results indicate only insignificant relativistic contributions to relative energies below 1.1 kcal mol^{-1} in all cases (cf. Table 4 below).

Reaction energies (ΔE) and reaction barriers ($\Delta E^{\ddagger}$) have been calculated from gas phase total energy differences; energies are given in kcal mol^{-1} relative to the sum of energies of the separated reactants $BBr_3 + HSiR_3$. We refrain from a discussion of enthalpies or free energies, which certainly alter computed barriers and reaction energies. But these contributions essentially reflect the quality of computed harmonic frequencies by the various methods, which is another issue outside our present focus.

3. Results and Discussion

The H/Br exchange by $HSiR_3$ according to eq 2 occurs via rate-limiting concerted transition states (cf. Figure 2).

CBS-QB3 results are used as reference throughout this study. As a supplementary consistency check we performed post-HF single-point calculations for the smallest model system with R = H. The results presented in Table 1 corroborate the choice of the CBS-QB3 extrapolation model as reference: deviations from the extrapolated (SCS)-MP2 and CCSD(T) basis set limit fall within the range of 1−2 kcal mol^{-1} generally considered as chemical accuracy and are of the same order as those observed in benchmark computations performed with the CBS-QB3 method for small silanes.[42,43] The use of CCSD(T)/cc-pVTZ optimized structures results in insignificant numerical differences in the extrapolated CCSD(T) basis set limit compared to the use of the inexpensive MP2/6-31G(d) level for geometry optimizations (below 0.1 kcal mol^{-1} maximum deviation).

Deviations of MP2 results from the CBS-QB3 reference data for all three systems are summarized in Table 2. The small 6-31G(d) basis allows for very efficient geometry optimizations but the resulting relative energies show significant deviations from the reference data. Much better agreement is achieved with the larger cc-pVTZ basis set, and the minute deviations between MP2/cc-pVTZ//MP2/6-31G(d) single-point results and those based on MP2/cc-pVTZ optimized geometries validate the use of MP2/6-31G(d) geometries for single-point calculations.

Addition of diffuse functions present in the aug-cc-pVTZ basis, does not alter the picture significantly for the reaction

TABLE 1: Benchmark Calculations for Reaction Energies and Activation Energies for the Reaction $BBr_3 + SiH_4 \rightarrow$ [TS] $\rightarrow BHBr_2 + BrSiH_3$ (Total Energy Differences in kcal mol^{-1} Relative to Separated Reactants)[a]

	MP2		SCS-MP2		CCSD(T)	
	ΔE	$\Delta E^{\ddagger}$	ΔE	$\Delta E^{\ddagger}$	ΔE	$\Delta E^{\ddagger}$
aug-cc-pVDZ	−2.9	19.6	−3.8	22.6	−3.5	21.7
aug-cc-pVTZ	−4.7	16.6	−5.6	20.2	−5.6	18.8
aug-cc-pVQZ	−5.2	16.4	−6.1	20.1	−6.3	18.7
aug-cc-pV5Z	−5.5	16.3	−6.5	20.0	−6.6	
xtra(aug-DT)[b]	−4.9	15.3	−5.7	19.1	−5.9	17.6
xtra(aug-TQ)[b]	−5.5	16.1	−6.6	19.9	−6.9	18.4
xtra(aug-Q5)[b]	−5.7	16.3	−6.7	20.0	−6.9	
CBS-QB3[c]					−5.5	18.5

[a] Single-point energy calculations based on MP2/6-31G(d) optimized structures. [b] Extrapolation to the basis set limit (see computational details section). [c] ZPVE contributions subtracted from CBS-QB3 results for 0 K.

TABLE 2: CBS-QB3 Reference Energies (Boldface) and Deviations[a] of MP2 Results for Reaction Energies and Activation Energies Computed for the Reaction $BBr_3 + HSiR_3 \rightarrow$ [TS] $\rightarrow BHBr_2 + BrSiR_3$ (Total Energy Differences in kcal mol^{-1} Relative to Separated Reactants)

	R = H		R = CH_3		R = C_2H_5	
method	ΔE	$\Delta E^{\ddagger}$	ΔE	$\Delta E^{\ddagger}$	ΔE	$\Delta E^{\ddagger}$
CBS-QB3	**−5.5**	**18.5**	**−12.5**	**8.1**	**−14.1**	**4.3**
MP2/6-31G(d)	−1.7	2.2	−3.9	−0.7	−4.6	−2.6
MP2/cc-pVTZ[b]	0.8	0.3	1.2	0.5	1.2	0.2
MP2/cc-pVTZ[c]	0.8	0.4	1.1	0.8	1.1	0.4
MP2/aug-cc-pVTZ[c]	0.8	−2.0	0.6	−2.7	0.2	−3.7
SCS-MP2/cc-pVTZ[c]	−0.2	3.9	0.9	5.3	1.2	5.9
SCS-MP2/aug-cc-pVTZ[c]	−0.1	1.6	0.3	1.9	0.3	1.8
MP2/aug-cc-pVDZ[d]	2.5	0.9	1.0	−2.5	0.1	−4.2
MP2/aug-cc-pVTZ[d]	0.8	−1.1	0.7	−1.5	0.4	−1.9
MP2/aug-cc-pVQZ[d]	0.4	−1.1	0.7	−0.8	0.6	−0.8
MP2/xtra(aug-DT)[d,e]	0.6	−2.1	0.7	−2.0	0.4	−2.2
MP2/xtra(aug-TQ) [d,e]	0.1	−1.3	0.5	−0.7	0.6	−0.4
SCS-MP2/aug-cc-pVDZ[d]	1.6	3.5	0.7	1.0	0.0	−0.1
SCS-MP2/aug-cc-pVTZ[d]	−0.1	2.1	0.4	2.4	0.4	2.6
SCS-MP2/aug-cc-pVQZ[d]	−0.6	2.1	0.3	3.2	0.5	3.8
SCS-MP2/xtra(aug-DT) [d,e]	−0.2	1.3	0.3	2.0	0.4	2.4
SCS-MP2/xtra(aug-TQ) [d,e]	−1.0	2.0	0.1	3.4	0.5	4.3

[a] Obtained as $\Delta E - \Delta E_{CBS\text{-}QB3}$ and $\Delta E^{\ddagger} - \Delta E^{\ddagger}_{CBS\text{-}QB3}$. [b] Geometry optimizations performed with Gaussian 03 using energies and gradients from RI-MP2 calculations with Turbomole (see computational details section). [c] Turbomole RI-MP2 single point calculations on MP2/6-31G(d) structures. [d] Turbomole RI-MP2 single point calculations on B3LYP/TZVP structures. [e] Extrapolation method: see computational details section.

TABLE 3: CBS-QB3 Reference Energies (Boldface) and Deviations[a] of DFT Results for Reaction Energies and Activation Energies in kcal/mol

	R = H				R = CH_3				R = C_2H_5			
	ΔE		$\Delta E^{\ddagger}$		ΔE		$\Delta E^{\ddagger}$		ΔE		$\Delta E^{\ddagger}$	
	SVP	TZVP	SVP	TZVP	SVP	TZVP	SVP	TZVP	SVP	TZVP	SVP	TZVP
CBS-QB3	**−5.5**		**18.5**		**−12.5**		**8.1**		**−14.1**		**4.3**	
BP86	3.6	1.0	3.1	2.1	4.9	2.4	6.2	5.5	5.4	3.2	7.8	7.4
BLYP	3.1	0.1	8.4	7.3	4.9	1.8	11.5	10.8	5.5	3.0	13.4	13.2
PW91	3.9	1.2	0.4	−0.7	5.0	2.4	2.8	2.2	5.2	3.1	4.0	3.9
PBE	4.0	1.3	0.7	−0.5	5.2	2.5	3.3	2.5	5.5	3.3	4.6	4.3
B3LYP[b]	2.0	−0.9	8.2	7.1	3.7	0.7	10.9	10.1	4.2	1.7	12.6	12.2
X3LYP[b]	2.1	−0.9	7.6	6.4	3.6	0.6	9.9	9.0	4.0	1.5	11.5	11.1
B2PLYP[b]	1.9	−1.1	7.1	4.9	3.3	0.0	8.8	6.7	3.6	0.7	9.9	8.1
B98	1.8	−0.9	4.9	3.7	3.3	0.5	7.4	6.5	3.7	1.4	8.9	8.5
M05	1.3	−1.3	5.3	4.4	2.7	0.0	7.6	6.7	3.1	0.8	8.9	8.5
BMK	0.7	−2.1	3.3	2.6	1.6	−1.0	5.2	4.4	1.9	−0.6	6.0	5.7
BB1K	1.8	−0.9	2.3	1.4	2.9	0.3	4.9	4.1	3.0	0.9	5.5	5.3
PBE0	2.5	−0.1	1.8	0.5	3.6	1.0	4.1	3.2	3.9	2.3	5.4	4.9
mPWB1K	1.8	−0.9	1.2	0.2	2.8	0.1	3.5	2.6	2.8	0.7	3.7	3.6
M05−2X	−0.6	−3.5	0.7	−0.7	−0.6	−3.4	−0.1	−1.3	−0.9	−3.3	−0.1	−0.8

[a] Obtained as $\Delta E - \Delta E_{\text{CBS-QB3}}$ and $\Delta E^{\ddagger} - \Delta E^{\ddagger}_{\text{CBS-QB3}}$. [b] B3LYP/X3LYP/B2PLYP: RI/RIJONX calculations with Orca, employing a *Gau_external* module for geometry optimizations (see computational details section).

energies, but barrier heights are now underestimated by 2−4 kcal mol^{-1} and deviations rise with growing size of R. The SCS-MP2/cc-pVTZ single-point results, in turn, show significantly overestimated barriers (by 4−6 kcal mol^{-1}) and deviations are reduced to 1.6−1.8 kcal mol^{-1} at the SCS-MP2/aug-cc-pVTZ level. The deviations of the SCS-MP2/cc-pVTZ single-point results are increasing with the size of R, while those obtained at the SCS-MP2/aug-cc-pVTZ level are nearly constant. The use of B3LYP/TZVP optimized structures for subsequent MP2/aug-cc-pVTZ single-point calculations leads to slightly improved agreement with the reference data (−1.9 kcal mol^{-1} maximum deviation) compared to the corresponding results based on MP2/6-31G(d) geometries (−3.7 kcal mol^{-1} maximum deviation). This is probably a consequence of the fact that the CBS-QB3 reference data is based on B3LYP geometries employing the CBSB7 basis of doubly polarized valence triple-ζ quality, which more closely resemble B3LYP/TZVP structures than those obtained at the MP2/6-31G(d) level.

Up to this point, these findings are in line with the perception that MP2 theory overestimates correlation energies quite generally. MP2 theory can profit from error compensation if used in combination with moderately sized basis sets (basis set incompleteness can effectively compensate the overestimation of correlation effects).[81] The spin component scaling in SCS-MP2 is designed to reduce this inherent overestimation of correlation energies. For both methods the use of diffuse functions consistently lowers the computed barriers by 2−4 kcal mol^{-1}, depending on the system size. For MP2, which yields barrier heights that agree within 1.1 kcal mol^{-1} with the reference values if used with the smaller cc-pVTZ basis, larger deviations result upon augmentation of the basis. SCS-MP2, on the other hand, profits from the use of augmented basis sets. In this case, we find that the spin-component scaling works as intended and SCS-MP2 is superior over standard MP2 if augmented basis sets are used.

A somewhat different picture arises, however, comparing the MP2 and SCS-MP2 basis set limit results (based on B3LYP/TZVP geometries, cf. Table 2). For MP2 theory, the inexpensive aug-DT-extrapolation achieves an acceptable agreement with the CBS-QB3 results to within −2.2 kcal mol^{-1}, and the extrapolated MP2/aug-TQ results show the best performance here (maximum deviation −1.3 kcal mol^{-1}). In contrast we find that the extrapolated SCS-MP2/aug-DT results overestimate the barrier heights by up to +2.4 kcal mol^{-1} and the aug-TQ extrapolation leads to even worse agreement with the reference data (maximum deviation +4.3 kcal mol^{-1}). These results indicate that the scaling factors employed in SCS-MP2 computations might not be optimal for a balanced description of the reaction studied here. We note in passing that others have applied different strategies to scale individual correlation components, including the pragmatic development of individual scaling factors optimized for different chemical applications.[82−84]

To assess the performance of DFT for these systems, geometry optimizations were performed with various functionals in combination with the SVP and TZVP basis sets. Table 3 shows the deviations of DFT results from the CBS-QB3 reference data.

For the reaction energies all GGAs show a more or less similar performance, underestimating the product stabilities by up to 5.5 kcal mol^{-1} in combination with the SVP basis, and the deviations slightly increase with the size of alkyl groups present at the silane. Systematically reduced errors generally result employing the larger TZVP basis. The BLYP functional performs like the other three GGAs for the reaction energies but it falls short for the barrier heights: with a notable error of 7 kcal mol^{-1} it shows the worst performance already for the smallest molecular model (R = H) and with enormous deviations of +10.8 to +13.2 kcal mol^{-1} (TZVP basis) it fails dramatically to describe the reaction barriers for the reactions with trimethyl- and triethylsilane. Also the BP86 functional shows significant deviations but for the smallest system. In striking contrast, the PW91 and PBE GGAs show significantly reduced errors that increase only moderately with the system size.

Turning to the hybrid functionals, we note that inclusion of 20% exact exchange in the B3LYP hybrid functional significantly improves the performance for reaction energies compared to the BLYP GGA. The corresponding B3LYP/TZVP results agree within 2 kcal mol^{-1} with the reference data so that these deviations fall within the estimated error margins of the CBS-QB3 method itself (cf. Table 1). For the largest molecular model, however, the reaction barrier is overestimated by 12.6 kcal mol^{-1}. Thus, the B3LYP hybrid fails nearly as dramatically for the barrier heights as the BLYP GGA does, closely followed

TABLE 4: CBS-QB3 Reference Energies (Boldface) and Deviations[a] of DFT Results for Reaction Energies and Activation Energies in kcal/mol

	R = H				R = CH_3				R = C_2H_5			
	ΔE		$\Delta E^{\ddagger}$		ΔE		$\Delta E^{\ddagger}$		ΔE		$\Delta E^{\ddagger}$	
	SVP	TZVP	SVP	TZVP	SVP	TZVP	SVP	TZVP	SVP	TZVP	SVP	TZVP
CBS-QB3	**−5.5**		**18.5**		**−12.5**		**8.1**		**−14.1**		**4.3**	
BLYP	3.1	0.1	8.4	7.3	4.9	1.8	11.5	10.8	5.5	3.0	13.4	13.2
PW91LYP	3.7	0.5	4.9	3.8	5.0	1.8	6.7	6.3	5.3	2.6	7.8	8.1
mPW91PW91	2.1	−0.4	3.1	2.0	3.4	1.0	5.8	5.1	3.8	1.8	7.3	7.1
BPW91	3.3	0.8	4.0	3.1	4.9	2.5	7.7	7.1	5.5	3.6	9.7	9.5
PW91	3.9	1.2	0.4	−0.7	5.0	2.4	2.8	2.2	5.2	3.1	4.0	3.9
B3LYP[b]	2.0	−0.9	8.2	7.1	3.7	0.7	10.9	10.1	4.2	1.7	12.6	12.2
BHandHLYP	0.4	−2.6	9.3	8.0	1.9	−1.1	11.3	10.2	2.3	−0.2	12.8	12.2
B3PW91	2.2	−0.3	4.5	3.5	3.6	1.2	7.7	7.0	4.2	2.1	9.5	9.1
PW3PW91	2.7	0.0	1.9	0.8	3.8	1.1	4.1	3.4	4.0	1.9	5.3	5.1
PBE-D[b]	4.0	1.2	−2.6	−3.6	4.2	1.5	−2.4	−3.1	3.7	1.6	−3.2	−3.3
B3LYP-D[b]	2.0	−1.0	4.2	3.1	2.3	−0.6	3.3	2.6	1.9	−0.5	2.1	2.1
B2PLYP-D[b]	1.9	−1.1	4.8	2.7	2.7	−0.6	4.7	2.7	2.4	−0.5	4.1	2.6
DKH2-B2LYP-D[b]	2.2	−0.4	4.9	3.6	2.5	−0.4	4.1	3.0	2.1	−0.5	3.0	2.4

[a] Obtained as $\Delta E - \Delta E_{\text{CBS-QB3}}$ and $\Delta E^{\ddagger} - \Delta E^{\ddagger}_{\text{CBS-QB3}}$. [b] B3LYP/X3LYP/B2PLYP: RIJONX calculations with Orca, employing a *Gau_external* module for geometry optimizations (see computational details section).

by the X3LYP, B2PLYP, B98, M05 functionals (in the order of decreasing errors), all of which overestimate the barriers substantially. In all these cases, deviations increase with the size of the silanes.[85]

Better players in the field are the functionals BMK, BB1K, and PBE0; the former two have specifically been devised to provide an optimal description of barrier heights[19,58,86] - but deviations of 5−6 kcal mol^{-1} for the largest system are unacceptable for the prediction of chemical kinetics. Replacement of B88 by mPW exchange in the mPWB1K functional yields further systematic improvements. By far the best performance is observed for the M05−2X functional, in particular if used with the smaller SVP basis. In contrast, use of the larger TZVP basis deteriorates the performance of this functional by 0.7−2.9 kcal mol^{-1}. The superior performance of M05−2X in combination with the smaller SVP basis might be related to the fact that a similarly small basis set has been used to some extent during the parametrization of M05−2X.[34] Further inspection of the data compiled in Table 3 reveals that a change from the SVP to the TZVP basis set results in a systematic shift of the computed reaction energies by −2.6 to −3.1 kcal mol^{-1}, i.e., to larger product stability for all three systems investigated. This shift is almost constant and independent of the functional employed. We discuss the influence of basis set limitations on the B2PLYP performance further below. We also explored the peculiar basis set dependence of the M05−2X functional in some more detail (the full set of data is provided as Supporting Information). Suffice it here to state that its performance with larger basis sets appears somewhat inconsistent, and it is only the M05−2X/SVP level which yields particularly good agreement with the reference data.

The large increase of errors for the computed barrier heights with the system size led us to speculate about the neglect of the increasing dispersive interactions in the transition structures as a fundamental source of error. The fact that we find the largest errors for functionals that incorporate the B88 exchange functional is reminiscent of earlier studies in which this functional failed to describe the binding in van der Waals-type rare gas dimers.[87−89] We also note that the correlation of DFT errors (in particular B3LYP) with system size was found earlier by Wodrich et al.[26,27] To further assess the origins of problems surfacing here we performed some additional calculations (Table 4).

Replacement of the B88 exchange functional by PW91 in the somewhat unusual functional combination PW91LYP leads to a system-dependent reduction of errors compared to the BLYP results, ranging from 3.5 kcal mol^{-1} (R = H) to 5.6 kcal mol^{-1} (R = Et) for barrier heights (see Table 4). The modifications of the PW91 exchange functional introduced by Adamo and Barone[50] to improve its performance for van der Waals interactions do not act in the desired direction here, but deteriorate the performance of mPW91PW91 compared to the parent PW91 GGA. A comparison of BLYP and BPW91 results reveals that the LYP correlation functional also inflicts significant errors on the computed barrier heights, quite constantly increasing the barriers by 3.7 to 4.4 kcal mol^{-1}, irrespective of basis set or system size. In line with our findings for the GGAs, constantly improved barriers result upon replacement of the LYP correlation functional in B3LYP by PW91. A slightly smaller effect results for the performance of the resulting B3PW91 hybrid, with barriers lowered by 3.1 to 3.7 kcal mol^{-1} compared to B3LYP. This, however, approximately corresponds to the reduced admixture (72%) of the LYP correlation component to the B3LYP hybrid, which now is replaced by PW91. Ad-hoc introduction of PW91 exchange to yield a PW3PW91 hybrid improves the results further, lowering the barrier heights again by 2.6−4.2 kcal mol^{-1} compared to B3PW91. While the admixture of exact HF exchange clearly enhances the performance for reaction energies, this is not true for the barrier heights calculated with the PW3PW91 hybrid, which does not quite reach the quality of the pure PW91 GGA. Furthermore, an increase of 20% exact exchange in the B3LYP functional to 50% in the BHandHLYP hybrid hardly shows any effect on the results and the computed barrier heights are particularly insensitive in this respect.

At this point the results provide evidence that both the B88 functional for exchange as well as the LYP functional for correlation cause substantial errors for the computed barrier heights. The fact that the B88 performance markedly deteriorates with increasing system size points to the presence of strong stabilizing dispersive interactions in the transition states of the larger systems. We thus performed further calculations including Grimme's empirical dispersion correction (Table 4), which indeed improves the performance of the B3LYP hybrid dramatically: the B3LYP-D results for the alkylated systems agree within 2−3 kcal mol^{-1} with the reference data. While the

TABLE 5: CBS-QB3 Reference Energies (Boldface) and Deviations[a] of B2PLYP Single-Point Results Based on B3LYP/TZVP Geometries for Reaction Energies and Activation Energies (in kcal mol^{-1}; B2PLYP-D Results Including Empirical Dispersion Corrections in Parentheses)

	R = H		R = CH_3		R = C_2H_5	
method	ΔE	$\Delta E^{\ddagger}$	ΔE	$\Delta E^{\ddagger}$	ΔE	$\Delta E^{\ddagger}$
CBS-QB3	**−5.5**	**18.5**	**−12.5**	**8.1**	**−14.1**	**4.3**
B2PLYP(-D)/cc-pVTZ	−0.4 (−0.5)	4.4 (2.3)	0.9 (0.2)	6.4 (2.5)	1.4 (0.1)	7.6 (2.5)
B2PLYP(-D)/aug-cc-pVDZ	0.9 (0.8)	4.2 (2.0)	0.9 (0.2)	3.8 (−0.1)	1.0 (−0.3)	4.0 (−1.2)
B2PLYP(-D)/aug-cc-pVTZ	−0.2 (−0.3)	2.1 (0.0)	0.2 (−0.5)	3.0 (−0.8)	0.3 (−1.0)	3.4 (−1.8)
B2PLYP(-D)/aug-cc-pVQZ	−0.4 (−0.4)	3.1 (0.9)	0.5 (−0.1)	4.6 (0.7)	0.9 (−0.4)	5.4 (0.2)
B2PLYP(-D)/xtra(aug-DTQ)[b]	−0.5 (−0.5)	3.8 (1.7)	0.8 (0.1)	5.6 (1.7)	1.3 (0.0)	6.8 (1.6)
B2PLYP(-D)/xtra(aug-DT)[c]	−0.7 (−0.7)	1.3 (−0.9)	−0.1 (−0.8)	2.7 (−1.1)	0.0 (−1.3)	3.2 (−2.0)
B2PLYP(-D)/xtra(aug-TQ)[c]	−0.5 (−0.6)	3.8 (1.7)	0.8 (0.1)	5.7 (1.8)	1.3 (0.0)	6.9 (1.7)
B2PLYP-CBS(-D)/SVP[d]	0.7 (0.7)	6.3 (4.1)	1.2 (0.5)	7.7 (3.9)	1.9 (0.6)	8.1 (2.9)
B2PLYP-CBS(-D)/TZVP[d]	−2.3 (−2.3)	4.3 (2.1)	−2.3 (−3.0)	5.2 (1.4)	−0.3 (−1.6)	6.3 (0.5)

[a] Obtained as $\Delta E - \Delta E_{\text{CBS-QB3}}$ and $\Delta E^{\ddagger} - \Delta E^{\ddagger}_{\text{CBS-QB3}}$. [b] 3-point extrapolation. [c] 2-point extrapolation (see computational details section). [d] Single-point energies at B3LYP/TZVP geometries, performed using Gaussian 03, CBS extrapolation scheme for MP2 correlation energy was used.

dispersion corrections lower the barrier by 4.0 kcal mol^{-1} for the smallest system (R = H), the corresponding contributions for the systems with R = Me and R = Et amount to enormous −7.5 and −10.5 kcal mol^{-1}, respectively. The remaining errors of the B3LYP-D functional for activation energies fall within the range of 2.1 to 4.2 kcal mol^{-1}, and the largest B3LYP-D error now occurs for the smallest molecular model. Unlike B3LYP, the PBE functional does not profit from dispersion corrections. The PBE-D results show errors of the same size as the pure PBE functional, but with an opposite sign, i.e., now the barriers are underestimated systematically. The small global scaling factor used to admix the empirical dispersion corrections to the PBE-D functional ($s_6 = 0.75$ compared to, e.g., 1.2 for BLYP and 1.05 for B3LYP)[60] indicates that the pure GGA already accounts for dispersion-like interactions to some extent. The present results might be taken as an indication that the empirical dispersion corrections employed are slightly too attractive (i.e., that the scaling factor for PBE-D is still too large), eventually overcompensating inherent PBE errors.

The notion of significant dispersive interactions stabilizing the transition states with increasing system size is corroborated by the poor performance of the B2PLYP double hybrid functional for barrier heights of the alkylated systems reported in Table 3. This functional has been designed to cover correlation effects at intermediate interelectronic distances and it has been validated very successfully in this context.[24] However, as detailed earlier by Schwabe and Grimme,[24,90] the amount of perturbative correction admixed (27%) does not suffice for an accurate account of long-range dispersive interactions and in careful calibration studies these authors found considerably improved results after adding an empirical dispersion correction tailored for the B2PLYP double hybrid. In perfect agreement with these studies, we find here that the B2PLYP-D composite performs substantially better than the B2PLYP functional itself: Reaction energies are shifted merely by 0.0−1.2 kcal mol^{-1} upon inclusion of dispersion corrections, whereas the errors for barrier heights are reduced by 2.2−5.8 kcal mol^{-1}.

The B2PLYP-D functional performs consistently better if used in combination with the larger TZVP basis set (cf. Table 4) but deviations from the reference values for activation energies still reach 2.7 kcal mol^{-1}. While the introduction of MP2-like perturbative correlation corrections insinuates a pronounced dependence of the performance of double hybrid functionals on basis set quality, Martin and co-workers[36] have pointed out that the effects of basis set limitations might effectively be compensated by the particular choice of coefficients that determine the amount of HF or MP2 admixed to the DFT part. In addition, as the global scaling factor of the empirical dispersion correction (s_6) is individually optimized for each functional, also these contributions indirectly depend on a specific basis set chosen in the parametrization procedure. Because basis sets of quadruple-ζ quality were employed during the setup of the B2PLYP functional components,[59] we performed further calculations to assess the influence of basis set quality on the B2PLYP-D functional performance.

To this end we performed single-point calculations on B3LYP/TZVP structures with Dunning's aug-cc-pV{D,T,Q}Z correlation-consistent basis set series and we applied various extrapolation procedures to estimate the basis set limit. Following a suggestion of Martin and co-workers[36] we also used Petersson's CBS procedure[91−94] to extrapolate the MP2 correlation energy contributions only. Since the results showed a significant dependence on the specific type of localization procedure applied, we employed the default settings of the CBS scheme. This procedure (referred to as B2PLYP-CBS/SVP and B2PLYP-CBS/TZVP in Table 5) results in a systematic shift to lower barriers and more exothermic reaction energies, eventually improving agreement with the reference on average by 1.5 and 0.5 kcal mol^{-1} for the SVP and TZVP basis, respectively. It is obvious, however, that the overall B2PLYP-CBS performance is inferior to extrapolations based on total energies.

The data compiled in Table 5 clearly shows that the B2PLYP functional performance improves only insignificantly with the basis set quality. Even at the basis set limit the agreement with the reference data is only marginally better than the TZVP results (Table 3). The most obvious improvement is seen upon augmentation of the basis set by diffuse functions and the aug-cc-pVDZ and aug-cc-pVTZ basis sets yield the best performance. Yet, worse agreement is seen at the basis set limit. As noted before, it is again the inclusion of empirical dispersion corrections that is crucial to achieve a reasonable agreement with the CBS-QB3 reference data: quite independent of the basis set, a pleasing overall performance is seen for the B2PLYP-D functional. The maximum deviation is reduced to 2.5 kcal mol^{-1} for the nonaugmented cc-pVTZ basis, and use of the very large aug-cc-pVQZ basis results in a very satisfying agreement within 1.0 kcal mol^{-1} with the reference data. Slightly larger errors occur, however, at the extrapolated basis set limit (up to 1.7−2.0

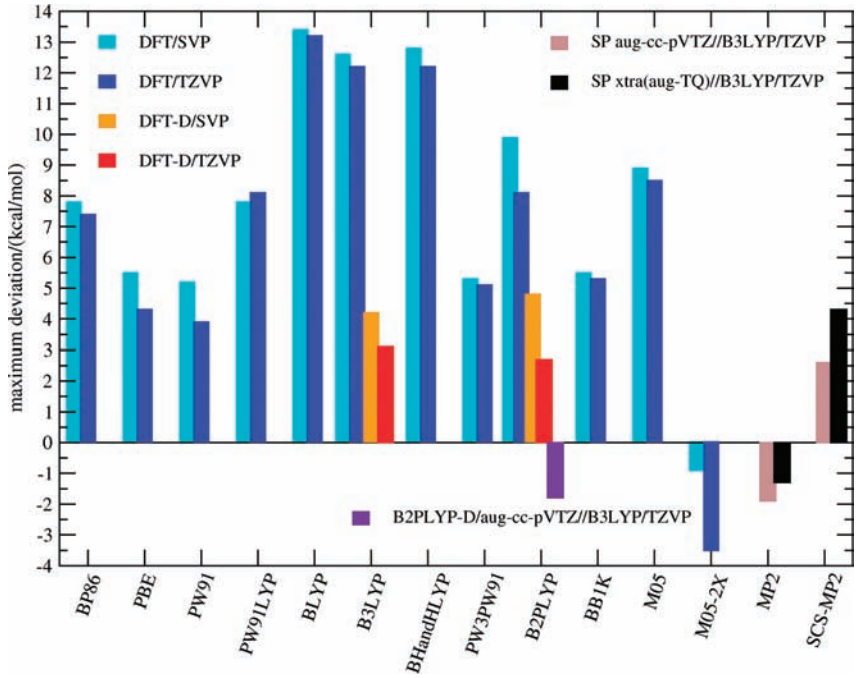

Figure 3. Overview of maximum deviations of DFT and (SCS-)MP2 results from the CBS-QB3 reference data (SP: single point calculation).

kcal mol^{-1}), which points to the fact that error compensation effects are responsible for the good performance of nonextrapolated results.

At this point we conclude that the B2PLYP-D functional performs best for the present set of systems if used in combination with the large aug-cc-pVQZ basis set. Although this excellent performance can be achieved employing B3LYP/TZVP geometries, we note that even single-point calculations at this level would be computationally too demanding for routine applications on significantly larger system sizes. Such basis set demands naturally limit the applicability of B2PLYP-D/aug-cc-pVQZ calculations to the same extent as they limit the applicability of (SCS-)MP2 theory, which also performs best if used in combination with large basis sets, as shown above. On the other hand, assuming an accuracy of about 2 kcal mol^{-1} for the CBS-QB3 reference method, an acceptable performance is found with basis sets of (augmented) triple-ζ quality. Irrespective of the choice of basis set, the empirical dispersion correction is the crucial component of the B3LYP-D and B2PLYP-D functionals to reduce the enormous errors for barrier heights in the present set of systems down to chemically reasonable limits.

4. Summary and Conclusion

In this study, we investigated the suitability of DFT and MP2 theory to explore the reactivity of organoboron species. We used the H/Br exchange reaction in BBr_3 with $HSiR_3$ ($R = H, CH_3, C_2H_5$) as a model system and CBS-QB3 as a reference method. By comparison of DFT and CBS-QB3 results, we have identified fundamental problems of many popular exchange-correlation functionals to properly describe the activation energy of the model reaction, while thermochemistry is described with significantly smaller errors by all methods employed (cf. Figure 3).

We provided evidence that both the B88 exchange and the LYP correlation functional components inflict particularly large errors cumulating in the BLYP GGA, which overestimates the barrier height of the largest model system by enormous 13.4 kcal mol^{-1}. The B3LYP hybrid functional, a highly efficient and reliable workhorse in many other research fields, also fails dramatically here with errors up to 12 kcal mol^{-1}. The PW91 GGA in turn, shows a fair agreement with the reference data to within 4 kcal mol^{-1}. The recently developed double hybrid functional B2PLYP still shows prominent errors up to 8 kcal mol^{-1} in combination with the standard TZVP basis, but its performance can be improved substantially employing the larger aug-cc-pVTZ basis set (2−3 kcal mol^{-1} deviation from the reference data). With deviations below 1 kcal mol^{-1}, however, the recently devised M05−2X hybrid functional performs excellently in combination with the small SVP basis set. The deviations found with larger basis sets suggest that this excellent agreement is a consequence of fortuitous error cancellation.

We have also identified the neglect of intramolecular dispersive interactions arising within the transition-state structures of the larger molecular models as the key problem of most functionals. The particularly prominent errors of the B3LYP and B2PLYP functionals can effectively be compensated by application of Grimme's empirical dispersion correction for DFT. The resulting B3LYP-D and B2PLYP-D composites perform within acceptable error limits (2−3 kcal mol^{-1}) for the present set of systems if used in combination with triple-ζ basis sets.

MP2 theory achieves an excellent agreement with the reference data if basis sets of at least triple-ζ quality are used. Best performance is found at the extrapolated basis set limit, which can be estimated effectively already by an inexpensive aug-DT extrapolation based on B3LYP/TZVP structures (deviations below 1 kcal mol^{-1}). Spin-component scaled MP2 yields a less satisfactory accuracy. Since (SCS-)MP2 theory can seriously fail for transition metal systems,[95] we suggest B2PLYP-D/aug-cc-pVTZ or B3LYP-D/TZVP as robust production level methods suitable for reactivity studies on systems such as that shown in Figure 1.[24,96]

Acknowledgment. Financial support by the DFG and by City Solar AG, Bad Kreuznach is acknowledged. We thank Profs. Matthias Wagner (Frankfurt) and Frank Neese (Bonn) for stimulating discussions.

Supporting Information Available: Comparison of the performance of different implementations of the B3LYP functional, of def-TZVP, def2-TZVP, and def2-TZVPP basis sets, and performance of the M05−2X functional with different basis sets. This material is available free of charge via the Internet at http://pubs.acs.org.

References and Notes

(1) Jäkle, F. *Coord. Chem. Rev.* **2006**, *250*, 1107.
(2) Miyata, M.; Chujo, Y. *Polym. J.* **2002**, *34*, 967.
(3) Welch, G. C.; San Juan, R. R.; Masuda, J. D.; Stephan, D. W. *Science* **2006**, *314*, 1124.
(4) Matsumi, N.; Naka, K.; Chujo, Y. *J. Am. Chem. Soc.* **1998**, *120*, 10776.
(5) Sundararaman, A.; Victor, M.; Varughese, R.; Jakle, F. *J. Am. Chem. Soc.* **2005**, *127*, 13748.
(6) Niu, W.; Smith, M. D.; Lavigne, J. J. *J. Am. Chem. Soc.* **2006**, *128*, 16466.
(7) Matsumi, N.; Naka, K.; Chujo, Y. *J. Am. Chem. Soc.* **1998**, *120*, 5112.
(8) Renk, T.; Ruf, W.; Siebert, W. *J. Organomet. Chem.* **1976**, *120*, 1.
(9) Scheibitz, M.; Bats, J. W.; Bolte, M.; Lerner, H. W.; Wagner, M. *Organometallics* **2004**, *23*, 940.
(10) Heilmann, J.; Scheibitz, M.; Qin, Y.; Sundararaman, A.; Jäkle, F.; Kretz, T.; Bolte, M.; Lerner, H.-W.; Holthausen, M. C.; Wagner, M. *Angew. Chem., Int. Ed.* **2006**, *45*, 920.
(11) Lorbach, A.; Bolte, M.; Li, H.; Lerner, H.-W.; Holthausen, M. C.; Jäkle, F.; Wagner, M. *Angew. Chem., Int. Ed.* **2009**, *45*, 4584.
(12) Heilmann, J. B.; Qin, Y.; Jäkle, F.; Lerner, H.-W.; Wagner, M. *Inorg. Chim. Acta* **2006**, *359*, 4802.
(13) Heilmann, J.; Scheibitz, M.; Qin, Y.; Sundararaman, A.; Jäkle, F.; Kretz, T.; Bolte, M.; Lerner, H.-W.; Holthausen, M. C.; Wagner, M. *Angew. Chem., Int. Ed.* **2006**, *45*, 920.
(14) Scheibitz, M.; Bolte, M.; Bats, J. W.; Lerner, H.-W.; Nowik, I.; Herber, R. H.; Krapp, A.; Lein, M.; Holthausen, M. C.; Wagner, M. *Chem.—Eur. J.* **2005**, *11*, 584.
(15) Koch, W.; Holthausen, M. C. *A Chemist's Guide to Density Functional Theory*, 2nd ed.; Wiley-VCH: Weinheim, Germany, 2001.
(16) Durant, J. L. *Chem. Phys. Lett.* **1996**, *256*, 595.
(17) Baker, J.; Andzelm, J.; Muir, M.; Taylor, P. R. *Chem. Phys. Lett.* **1995**, *237*, 53.
(18) Yi, S. S.; Reichert, E. L.; Holthausen, M. C.; Koch, W.; Weisshaar, J. C. *Chem.—Eur. J.* **2000**, *6*, 2232.
(19) Boese, A. D.; Martin, J. M. L. *J. Chem. Phys.* **2004**, *121*, 3405.
(20) Gilbert, T. M. *J. Phys. Chem. A* **2004**, *108*, 2550.
(21) Phillips, J. A.; Cramer, C. J. *J. Chem. Theory Comput.* **2005**, *1*, 827.
(22) Plumley, J. A.; Evanseck, J. D. *J. Phys. Chem. A* **2007**, *111*, 13472.
(23) Zhao, Y.; Truhlar, D. G. *Acc. Chem. Res.* **2008**, *41*, 157.
(24) Schwabe, T.; Grimme, S. *Acc. Chem. Res.* **2008**, *41*, 569.
(25) Schreiner, P. R. *Angew. Chem., Int. Ed.* **2007**, *46*, 4217.
(26) Wodrich, M. D.; Corminboeuf, C.; Schleyer, P. v. R. *Org. Lett.* **2006**, *8*, 3631.
(27) Wodrich, M. D.; Corminboeuf, C.; Schreiner, P. R.; Fokin, A. A.; Schleyer, P. v. R. *Org. Lett.* **2007**, *9*, 1851.
(28) Grimme, S. *Angew. Chem., Int. Ed.* **2006**, *45*, 4460.
(29) Elstner, M.; Hobza, P.; Frauenheim, T.; Suhai, S.; Kaxiras, E. *J. Chem. Phys.* **2001**, *114*, 5149.
(30) Wu, X.; Vargas, M. C.; Nayak, S.; Lotrich, V.; Scoles, G. *J. Chem. Phys.* **2001**, *115*, 8748.
(31) Wu, Q.; Yang, W. *J. Chem. Phys.* **2002**, *116*, 515.
(32) Zimmerli, U.; Parrinello, M.; Koumoutsakos, P. *J. Chem. Phys.* **2004**, *120*, 2693.
(33) Grimme, S. *J. Comput. Chem.* **2004**, *25*, 1463.
(34) Zhao, Y.; Schultz, N. E.; Truhlar, D. G. *J. Chem. Theory Comput.* **2006**, *2*, 364.
(35) Xu, X.; Goddard, W. A., III *Proc. Natl. Acad. Sci.* **2004**, *101*, 2673.
(36) Tarnopolsky, A.; Karton, A.; Sertchook, R.; Vuzman, D.; Martin, J. M. L. *J. Phys. Chem. A* **2008**, *112*, 3.
(37) Karton, A.; Tarnopolsky, A.; Lamère, J.-F.; Schatz, G. C.; Martin, J. M. L. *J. Phys. Chem. A* **2008**, *112*, 12868.
(38) Frisch, M. J.; Trucks, G. W.; Schlegel, H. B.; Scuseria, G. E.; Robb, M. A.; Cheeseman, J. R.; Montgomery, J. A., Jr.; Vreven, T.; Kudin, K. N.; Burant, J. C.; Millam, J. M.; Iyengar, S. S.; Tomasi, J.; Barone, V.; Mennucci, B.; Cossi, M.; Scalmani, G.; Rega, N.; Petersson, G. A.; Nakatsuji, H.; Hada, M.; Ehara, M.; Toyota, K.; Fukuda, R.; Hasegawa, J.; Ishida, M.; Nakajima, T.; Honda, Y.; Kitao, O.; Nakai, H.; Klene, M.; Li, X.; Knox, J. E.; Hratchian, H. P.; Cross, J. B.; Adamo, C.; Jaramillo, J.; Gomperts, R.; Stratmann, R. E.; Yazyev, O.; Austin, A. J.; Cammi, R.; Pomelli, C.; Ochterski, J. W.; Ayala, P. Y.; Morokuma, K.; Voth, G. A.; Salvador, P.; Dannenberg, J. J.; Zakrzewski, V. G.; Dapprich, S.; Daniels, A. D.; Strain, M. C.; Farkas, O.; Malick, D. K.; Rabuck, A. D.; Raghavachari, K.; Foresman, J. B.; Ortiz, J. V.; Cui, Q.; Baboul, A. G.; Clifford, S.; Cioslowski, J.; Stefanov, B. B.; Liu, G.; Liashenko, A.; Piskorz, P.; Komaromi, I.; Martin, R. L.; Fox, D. J.; Keith, T.; Al-Laham, M. A.; Peng, C. Y.; Nanayakkara, A.; Challacombe, M.; Gill, P. M. W.; Johnson, B.; Chen, W.; Wong, M. W.; Gonzalez, C.; Pople, J. A. *Gaussian 03*, revision D.01; Gaussian, Inc.: Wallingford, CT, 2004.
(39) Werner, H.-J.; Knowles, P. J.; Lindh, R.; Manby, F. R.; Schütz, M.; Celani, P.; Korona, T.; Rauhut, G.; Amos, R. D.; Bernhardsson, A.; Berning, A.; Cooper, D. L.; Deegan, M. J. O.; Dobbyn, A. J.; Eckert, F.; Hampel, C.; Hetzer, G.; Lloyd, A. W.; McNicholas, S. J.; Meyer, W.; Mura, M. E.; Nicklass, A.; Palmieri, P.; Pitzer, R.; Schumann, U.; Stoll, H.; Stone, A. J.; Tarroni, R.; Thorsteinsson, T. MOLPRO Version 2006; 2006.1 ed., 2006.
(40) Ahlrichs, R.; Bär, M.; Baron, H. P.; Bauernschmitt, R.; Böcker, S.; Ehrig, M.; Eichkorn, K.; Elliott, S.; Furche, F.; Haase, F.; Häser, M.; Hättig, C.; Horn, H.; Huber, C.; Huniar, U.; Kattanek, M.; Köhn, A.; Kölmel, C.; Kollwitz, M.; May, K.; Ochsenfeld, C.; Öhm, H.; Schäfer, A.; Schneider, U.; Treutler, O.; Tsereteli, K.; Unterreiner, B.; Arnim, M. v.; Weigend, F.; Weis, P.; Weiss, H. *Turbomole*, version 5.10; Universität Karlsruhe: Germany, 2008.
(41) Neese, F. *Orca*, revision 2.6.35; Universität Bonn: Germany, 2008.
(42) Montgomery, J. J. A.; Frisch, M. J.; Ochterski, J. W.; Petersson, G. A. *J. Chem. Phys.* **1999**, *110*, 2822.
(43) Montgomery, J. J. A.; Frisch, M. J.; Ochterski, J. W.; Petersson, G. A. *J. Chem. Phys.* **2000**, *112*, 6532.
(44) Perdew, J. P. *Phys. Rev. B* **1986**, *33*, 8822.
(45) Becke, A. D. *Phys. Rev. A* **1988**, *38*, 3098.
(46) Lee, C.; Yang, W.; Parr, R. G. *Phys. Rev. B* **1988**, *37*, 785.
(47) Miehlich, B.; Savin, A.; Stoll, H.; Preuss, H. *Chem. Phys. Lett.* **1989**, *157*, 200.
(48) Perdew, J. P.; Chevary, J. A.; Vosko, S. H.; Jackson, K. A.; Pederson, M. R.; Singh, D. J.; Fiolhais, C. *Phys. Rev. B* **1992**, *46*, 6671.
(49) Perdew, J. P.; Chevary, J. A.; Vosko, S. H.; Jackson, K. A.; Pederson, M. R.; Singh, D. J.; Fiolhais, C. *Phys. Rev. B* **1993**, *48*, 4978.
(50) Adamo, C.; Barone, V. *J. Chem. Phys.* **1998**, *108*, 664.
(51) Stephens, P. J.; Devlin, F. J.; Chabalowski, C. F.; Frisch, M. J. *J. Phys. Chem.* **1994**, *98*, 11623.
(52) Becke, A. D. *J. Chem. Phys.* **1993**, *98*, 5648.
(53) Perdew, J. P.; Burke, K.; Ernzerhof, M. *Phys. Rev. Lett.* **1996**, *77*, 3865.
(54) Adamo, C.; Ernzerhof, M.; Scuseria, G. E. *J. Chem. Phys.* **2000**, *112*, 2643.
(55) Ernzerhof, M.; Scuseria, G. E. *J. Chem. Phys.* **1999**, *110*, 5029.
(56) Becke, A. D. *J. Chem. Phys.* **1998**, *109*, 2092.
(57) Zhao, Y.; Schultz, N. E.; Truhlar, D. G. *J. Chem. Phys.* **2005**, *123*, 161103.
(58) Zhao, Y.; Truhlar, D. G. *J. Phys. Chem. A* **2004**, *108*, 6908.
(59) Grimme, S. *J. Chem. Phys.* **2006**, *124*, 034108.
(60) Grimme, S. *J. Comput. Chem.* **2006**, *27*, 1787.
(61) Please note that in these calculations the B3LYP functional has been used in a slightly modified form implemented in TURBOMOLE and ORCA, which makes use of the local VWN5 correlation functional instead of the VWN3 functional employed in the GAUSSIAN program: see Hertwig, R. H.; Koch, W. *Chem. Phys. Lett.* **1997**, *268*, 345. The particular choice of functional, however, was found to cause insignificant changes in the computed results only (0.2 kcal/mol).
(62) Grimme, S. *J. Chem. Phys.* **2003**, *118*, 9095.
(63) Neese, F. *J. Comput. Chem.* **2003**, *24*, 1740.
(64) Neese, F.; Olbrich, G. *Chem. Phys. Lett.* **2002**, *362*, 170.
(65) Eichkorn, K.; Treutler, O.; Öhm, H.; Häser, M.; Ahlrichs, R. *Chem. Phys. Lett.* **1995**, *240*, 283.
(66) Eichkorn, K.; Weigend, F.; Treutler, O.; Ahlrichs, R. *Theor. Chem. Acc.* **1997**, *97*, 119.
(67) Weigend, F.; Häser, M.; Patzelt, H.; Ahlrichs, R. *Chem. Phys. Lett.* **1998**, *294*, 143.
(68) Rassolov, V. A.; Ratner, M. A.; Pople, J. A.; Redfern, P. C.; Curtiss, L. A. *J. Comput. Chem.* **2001**, *22*, 976.
(69) Schäfer, A.; Horn, H.; Ahlrichs, R. *J. Chem. Phys.* **1992**, *97*, 2571.
(70) Schäfer, A.; Huber, C.; Ahlrichs, R. *J. Chem. Phys.* **1994**, *100*, 5829.
(71) We have identified partly erroneous implementations of the standard SVP and TZVP basis sets for Br in ORCA up to version 2.6.35, i.e., faulty contraction coefficients and/or d-polarization exponents; these errors have been brought to the attention of the ORCA developers and are corrected in subsequent program versions.
(72) Dunning, T. H., Jr. *J. Chem. Phys.* **1989**, *90*, 1007.
(73) Wilson, A. K.; Woon, D. E.; Petersson, K. A.; Dunning, T. H, Jr. *J. Chem. Phys.* **1999**, *110*, 7667.
(74) Halkier, A.; Helgaker, T.; Jørgensen, P.; Klopper, W.; Koch, H.; Olsen, J.; Wilson, A. K. *Chem. Phys. Lett.* **1998**, *286*, 243.

(75) Helgaker, T.; Jørgensen, P.; Olsen, J. *Molecular Electronic-Structure Theory*; Wiley: Chichester, U.K., 2000.
(76) Peterson, K. A.; Woon, D. E.; Dunning, T. H, Jr. *J. Chem. Phys.* **1994**, *100*, 7410.
(77) Douglas, M.; Kroll, N. M. *Ann. Phys.* **1974**, *82*, 89.
(78) Hess, B. A. *Phys. Rev. A* **1985**, *32*, 756.
(79) Hess, B. A. *Phys. Rev. A* **1986**, *33*, 3742.
(80) Jansen, G.; Hess, B. A. *Phys. Rev. A* **1989**, *39*, 6016.
(81) Schwabe, T.; Grimme, S. *J. Chem. Phys. A* **2009**, *113*, 3005.
(82) Hill, J. G.; Platts, J. A. *J. Chem. Theor. Comput.* **2007**, *3*, 80.
(83) Distasio, R. A., Jr; Head-Gordon, M. *Mol. Phys.* **2007**, *105*, 1073.
(84) Zhao, Y.; Truhlar, D. G. *J. Chem. Theor. Comput.* **2009**, *5*, 324.
(85) A referee suggested the use of the newly devised def2-TZVP basis set (Weigend, F.; Ahlrichs, R. *Phys. Chem. Chem. Phys.* **2005**, *7*, 3297.) instead of the TZVP basis. We performed B3LYP/def2-TZVP and B3LYP/def2-TZVPP single-point calculations based on B3LYP/TZVP geometries and found only negligible differences for relative energies and barrier heights (deviations ranging from −0.5 to +0.8 kcal/mol, see Table S2, Supplementary information).
(86) Zhao, Y.; Lynch, B. J.; Truhlar, D. G. *J. Phys. Chem. A* **2004**, *108*, 2715.
(87) Zhang, Y.; Pan, W.; Yang, W. *J. Chem. Phys.* **1997**, *107*, 7921.
(88) Pérez-Jordá, J. M.; Becke, A. D. *Chem. Phys. Lett.* **1995**, *233*−134.
(89) Kristyán, S.; Pulay, P. *Chem. Phys. Lett.* **1994**, *229*, 175.
(90) Schwabe, T.; Grimme, S. *Phys. Chem. Chem. Phys.* **2007**, *9*, 3397.
(91) Nyden, M. R.; Petersson, G. A. *J. Phys. Chem.* **1981**, *75*, 1843.
(92) Petersson, G. A.; Bennett, A.; Tensfeldt, T. G.; Al-Laham, M. A.; Shirley, W. A.; Mantzaris, J. *J. Chem. Phys.* **1988**, *89*, 2193.
(93) Petersson, G. A.; Al-Laham, M. A. *J. Phys. Chem.* **1991**, *94*, 6081.
(94) Petersson, G. A.; Tensfeldt, T. G.; Montgomery, J. A, Jr. *J. Chem. Phys.* **1991**, *94*, 6091.
(95) Hyla-Kryspin, I.; Grimme, S. *Organometallics* **2004**, *23*, 5581.
(96) Piacenza, M.; Hyla-Kryspin, I.; Grimme, S. *J. Comput. Chem.* **2007**, *28*, 2275.

JP906502Y